Int. J. Electrochem. Sci., 9 **(2014)** 5204 - 5221

International Journal of
ELECTROCHEMICAL
SCIENCE
www.electrochemsci.org

Synergistic Inhibition between Benzyl Triphenyl Phosphonium Chloride and Halide Ions on the Corrosion of Mild Steel in Acidic Medium

H. Vashisht[1], *I. Bahadur*[2], *S. Kumar* [1,*], *G. Singh*[1], *D. Ramjugernath*[2,*], *E. E. Ebenso*[3]

[1]Department of Chemistry, University of Delhi, Delhi-110007
[2]Thermodynamics Research Unit, School of Engineering, University of KwaZulu-Natal, Howard College Campus, King George V Avenue, Durban, 4041, South Africa
[3]Department of Chemistry, North-West University (Mafikeng Campus), Private Bag X2046, Mmabatho 2735, South Africa
[*]E-mail: sudershankumar2005@gmail.com; ramjuger@ukzn.ac.za

Received: 25 February 2014 / *Accepted:* 29 May 2014 / *Published:* 16 June 2014

The effect of benzyl triphenyl phosphonium chloride (BTPPC) and halide ion (KI) on the corrosion of mild steel in a solution of 0.3 M phosphoric acid have been investigated at various inhibitor concentrations and temperatures by potentiodynamic polarization, electrochemical impedance spectroscopy (EIS), temperature kinetic, scanning electron microscopy (SEM) and atomic force microscopy (AFM) studies, respectively. Results obtained from potentiodynamic polarization studies, reveal that BTPPC and KI are mixed type inhibitors for mild steel in 0.3 M phosphoric acid. The synergistic effect of BTPPC and KI in corrosion inhibition of mild steel in 0.3 M H_3PO_4 containing low concentration of I^- has been evaluated by potentiodynamic polarization studies. The experimental results suggest that the presence of iodide ions in the solution stabilized the adsorption of BTPPC molecules on the metal surface and improved the inhibition efficiency of BTPPC. The corrosion behavior of mild steel in 0.3 M H_3PO_4 without and with the inhibitor at various concentrations was studied in the temperature range from (298 to 338) K. The inhibition efficiency increases with an increase in concentration at all temperatures. The inhibition efficiencies decrease with an increase in temperature. The adsorption of BTPPC + KI accords to the Temkin adsorption isotherm. Kinetic and thermodynamic parameters such as effective activation energy (E_a), Gibbs free energy of adsorption (ΔG^o_{ads}) and heat of adsorption (ΔH^o_{ads}) indicate that the adsorption of BTPPC + KI on the mild steel surface is primarily physical in nature. The results of scanning electron microscopy and atomic force microscopy are in agreement with the electrochemical analysis results.

Keywords: Polarization; Synergism; EIS; SEM; AFM

1. INTRODUCTION

Corrosion is the natural process of deterioration of metals and alloys in a corrosive environment. Corrosion occurs in a wide variety of forms, both in pure metals and in alloys. The use of inhibitors is one of the most practical methods to secure metal against acid corrosion. Many works have studied the influence of organic compounds containing nitrogen [1-10], sulfur [11-17], oxygen [18-20] and phosphorous [21-23] on the corrosion of mild steel in acidic media. The results show that most organic compounds employed as corrosion inhibitors can adsorb on the metal surface through heteroatom such as N, S, O, P and multiple bonds which prevent steel from corrosion. The inhibitive effect of inhibitors is attributed to the adsorption ability of the molecules onto the metal surface according to some known adsorption isotherm. This adsorption process affects the cathodic and anodic dissolution reactions to different extents. Anodic dissolution of steel has been extensively studied in acidic media and the mechanism of the process has been the subject in several papers. Phosphoric acid (H_3PO_4) is a medium–strong acid, but it still shows strong corrosiveness on ferrous or ferrous alloy [24]. Phosphoric acid is produced in large quantities in Morocco. It is widely used in industries such as the food industry, acid pickling, acid cleaning and acid descaling. Phosphonium compounds show biocidal properties against macro and micro-organisms e.g., bacteria, algae, and mollusks etc. Phosphonium compounds can also be used for the protection of technical materials, water systems, lubricants and other materials synergistic inhibition is an effective means to improve the inhibitive force of the inhibitor. The halides are the most effective derivatives because they increase the inhibiting tendency of the inhibitor by the well-known phenomenon of the synergistic effect [25-34]. In this study, the inhibition effect of BTPPC + KI for the corrosion of mild steel in 0.3 M H_3PO_4 solution has been studied by potentiodynamic polarization, potentiostatic polarization, electrochemical impedance spectroscopy (EIS), temperature kinetic, scanning electron microscopy (SEM), and atomic force microscopy (AFM) studies.

2. EXPERIMENTAL

2.1. Materials

The chemical composition, wt. % of mild steel, used in this study is given in Table 1.

Table 1. Composition of mild steel (wt. %).

C	*Si*	*S*	*P*	*Mn*	*Fe*
0.15	0.31	0.025	0.025	1.02	Balance

2.2 Solutions

All solutions were prepared from doubly distilled water and AR grade H_3PO_4 was used. The concentration range of inhibitor employed was (10^{-3} to 10^{-7}) M and concentration of KI employed was 10^{-3} M in 0.3 M phosphoric acid.

2.3 The structure of BTPPC

The organic additive, benzyl triphenyl phosphonium chloride $C_{25}H_{22}ClP$, $C_6H_5P\ \{C_6H_5\}_3\ Cl$ is used as the inhibitor. The structure of the inhibitor is shown in Figure 1. The inhibitor has the following physical properties, such as M.W. = 388.88g, Assay = 97% and M.P = 325-330 ^{O}C.

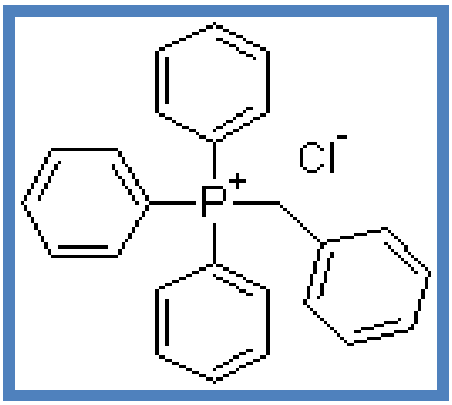

Figure 1. Molecular structure of BTPPC.

2.4 Electrochemical measurements

The working electrode (WE) for the potentiodynamic studies was cut from a mild steel rod and was soldered on one end with an insulated copper wire and it was then embedded in chemical epoxy resin (ARALDITE) leaving the exposed surface area of 0.9 cm^2 for experiment studies. The counter electrode was platinum and the reference was a saturated calomel electrode (SCE) coupled to a luggin capillary. The potential of the metal electrode versus reference electrode was measured with the help of a Galvanostat. A steady state potential was achieved in 4-5 hours. The electrode system used for electrochemical impedance spectroscopy was the same as the one used for potentiodynamic polarization studies. Potentiodynamic polarization measurements were performed using a electrochemical analyzer CHI 6021B under aerated conditions. Potentiodynamic anodic and cathodic polarization curves were obtained with a scan rate of $0.001Vs^{-1}$ in the potential range from -1.2V to 0.2V relative to the corrosion potential (E_{corr}). Electrochemical impedance spectroscopy was performed using a electrochemical analyzer CHI760C under aerated conditions. Impedance spectra were recorded at E_{corr} in the frequency range 100000Hz to 1Hz. The ac voltage amplitude was 0.005V.

Properly ground and polished samples of mild steel (1cm x 1cm x 1cm) were used for AFM and SEM. AFM measurements were performed using the VEECO CPII atomic force microscope model no. MPP-11123 using Resonance frequency f_o = 20-80 N/m and spring constant k = 20-80 N/m. The topographic images were measured by AFM applying force between the sample and Al- coated conductive tip.

SEM measurements were performed using a Leo 435 VP in high vacuum mode and equipped with digital imaging and 35 mm photography system. SEM images were obtained by a applying operative voltage of 15-30KV.

3. RESULTS AND DISCUSSION

3.1. Potentiodynamic polarization studies

In the present study, 0.3 M H_3PO_4 was used for the polarization of mild steel at five temperatures namely, (298, 308, 318, 328 and 338) K. The potential values are plotted in Figure 2 against the logarithm of current densities and various parameters were calculated from the graphs and are reported in Table 2.

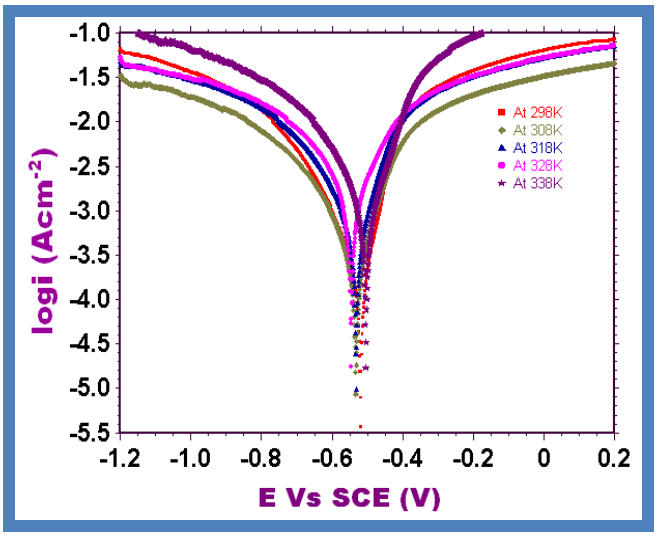

Figure 2. Tafel polarization curves of mild steel in 0.3 M H_3PO_4 at different temperatures.

Table 2. Corrosion Parameters of mild steel in 0.3 M H_3PO_4

T/(K)	$-E_{corr}$/(V)	b_c/(mV/dec)	b_a/(mV/dec)	i_{corr}/(A.cm^{-2}) × 10^4
298	0.519	2.395	2.568	8.09
308	0.533	2.316	2.455	10.85
318	0.532	3.157	3.077	16.11
328	0.545	2.252	2.280	27.20
338	0.505	1.838	2.911	36.96

An increase in the corrosion current values for 0.3 M H_3PO_4 is observed with an increase in temperatura, thereby indicating that the extent of corrosion increases with an increase in temperature. E_{corr} remains almost constant with an increase in temperature. Anodic and cathodic Tafel slopes remain almost constant with temperature and $b_c \approx b_a$.

Solutions of various concentrations of BTPPC + KI were prepared in 0.3 M H_3PO_4, namely (10^{-3}, 10^{-5} and 10^{-7}) M and a concentration of 10^{-3}M KI, which were then used for the polarization studies. Potential values were plotted against the logarithm of current densities and various parameters were calculated which are given in Table 3.

Table 3. Corrosion Parameters of mild steel in 0.3 M H_3PO_4 in the presence of BTPPC + 10^{-3}M KI

T/(K)	*Conc.* / (M)	$-E_{corr}$ / (V)	b_c / (mV/dec)	b_a / (mV/dec)	i_{corr} / (A/cm^2)×10^5	*I%*
298	10^{-3}	0.521	2.699	3.513	3.95	95.12
	10^{-5}	0.529	3.022	3.091	5.33	93.41
	10^{-7}	0.509	5.416	7.477	17.73	78.09
	H_3PO_4	0.519	2.395	2.568	80.92	
308	10^{-3}	0.502	2.726	4.021	5.186	95.22
	10^{-5}	0.509	2.972	3.357	14.96	86.21
	10^{-7}	0.523	3.034	3.143	26.13	75.91
	H_3PO_4	0.533	2.316	2.455	108.50	
318	10^{-3}	0.531	3.411	4.132	10.70	93.36
	10^{-5}	0.507	4.019	4.023	388.00	75.91
	10^{-7}	0.528	4.640	5.746	402.20	75.16
	H_3PO_4	0.532	3.157	3.077	161.10	
328	10^{-3}	0.497	4.199	5.371	23.59	91.33
	10^{-5}	0.508	2.122	2.941	69.48	74.45
	10^{-7}	0.529	4.328	4.770	91.32	67.77
	H_3PO_4	0.545	2.252	2.820	272.00	
338	10^{-3}	0.529	2.391	3.297	32.48	91.21
	10^{-5}	0.504	2.119	2.396	129.00	65.09
	10^{-7}	0.520	1.822	2.669	187.40	49.29
	H_3PO_4	0.505	1.838	2.911	369.60	

Figure 3 gives the cathodic and anodic polarization curves for these solutions at 298 K.

The inhibition efficiency was calculated using the following expression [35]:

$$I\% = \left(\frac{i_o - i}{i_o}\right) \times 100 \quad (1)$$

where i_o is the corrosion current in the uninhibited solution and i is the corrosion current in the inhibited solution. The corrosion currents decrease by a large extent in the presence of BTPPC + 10^{-3} M KI as compared to pure acid. The decrease in i_{corr} is more pronounced at room temperature as compared to higher temperatures.

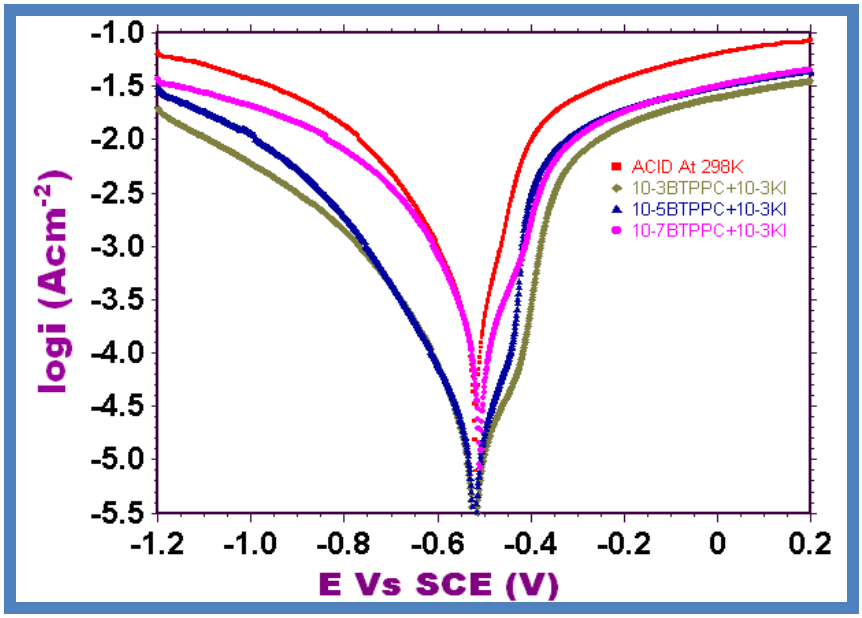

Figure 3. Tafel polarization curves of mild steel in 0.3 M H_3PO_4 and in the presence of BTPPC + 10^{-3}M KI at 298 K.

The inhibition efficiency is a maximum for 10^{-3} M BTPPC + 10^{-3} M KI concentrations and it remains almost constant with an increase in temperature, thereby indicating that the inhibition is efficient at all the temperatures. As the concentration is lowered to 10^{-5} M BTPPC + 10^{-3} M KI and 10^{-7} M BTPPC + 10^{-3} M KI, the inhibition efficiency decreases with an increase in temperature. The values of b_c and b_a are found to be higher in the presence of the additives than in pure acid. Adsorption may be the key mechanism involved in the inhibition process. At all concentrations and temperatures studied, $b_c \approx b_a$. E_{corr} is almost constant indicating that the additives act like a mixed type inhibitor blocking both cathodic and anodic reactions to an equal extent.

3.2. Synergistic Parameter

Aramaki and Hackermann [36] calculated the synergism parameter S_Θ using the following equation:

$$S_{\Theta} = \frac{1-\Theta_{1+2}}{1-\Theta'_{1+2}} \quad (2)$$

where $\Theta_{1+2} = (\Theta_1 + \Theta_2) - (\Theta_1 . \Theta_2)$

Θ_1 is the surface coverage by the anion

Θ_2 is the surface coverage by the cation

Θ'_{1+2} is measured surface coverage by both the anion and cation.

The synergism parameter is calculated from the equation above. The comparative corrosion inhibition values of BTPPC [37] and BTPPC + KI are given in Table 4 and the corresponding values of synergism parameter (S_{Θ}) of BTPPC are given in Table 5.

Table 4. Comparative table of corrosion inhibition of mild steel in 0.3 M H_3PO_4 in the presence of BTPPC only and in the presence of BTPPC + 10^{-3}M KI

T/(K)	*Conc.*/(M)	i_{corr}/(A/cm^2) × 10^5 (BTPPC)	*I%* (BTPPC)	i_{corr} /(A/cm^2)×10^5 (BTPPC + KI)	*I%* (BTPPC + KI)
298	10^{-3}	4.67	94.23	3.95	95.12
	10^{-5}	10.55	86.96	5.33	93.41
	10^{-7}	39.42	51.28	17.73	78.09
	H_3PO_4	80.92		80.92	
308	10^{-3}	12.97	88.05	5.186	95.22
	10^{-5}	38.47	64.54	14.96	86.21
	10^{-7}	64.03	40.98	26.13	75.91
	H_3PO_4	108.50		108.50	
318	10^{-3}	61.76	61.66	10.70	93.36
	10^{-5}	110.80	31.22	388.00	75.91
	10^{-7}	114.10	29.17	402.20	75.16
	H_3PO_4	161.10		161.10	
328	10^{-3}	44.06	83.88	23.59	91.33
	10^{-5}	199.00	26.38	69.48	74.45
	10^{-7}	224.30	17.53	91.32	67.77
	H_3PO_4	272.00		272.00	
338	10^{-3}	54.97	85.13	32.48	91.21
	10^{-5}	331.4	10.33	129.00	65.09
	10^{-7}	348.90	5.64	187.40	49.29
	H_3PO_4	369.60		369.60	

As can be seen from Table 5, synergism values exceed unity at 298 K, and from Table 4 it can be seen the increase of inhibition efficiencies on the addition of the halide ion which suggests that the enhanced inhibition efficiencies caused by the addition of iodide ions to BTPPC is due to the synergistic effect [33] only. This synergistic inhibition brought by the combination of BTPPC + KI for the corrosion of mild steel in 0.3 M H_3PO_4 can be explained as follows.

Table 5. Synergism parameter (*S*ϴ) for various concentrations of BTPPC

T / (K)	*Conc.* / (M)	*S*ϴ
298	10^{-3}	1.02
	10^{-5}	1.01
	10^{-7}	1.02
308	10^{-3}	1.01
	10^{-5}	0.84
	10^{-7}	1.08
318	10^{-3}	0.71
	10^{-5}	0.47
	10^{-7}	0.49
328	10^{-3}	0.94
	10^{-5}	0.51
	10^{-7}	0.45
338	10^{-3}	0.94
	10^{-5}	0.24
	10^{-7}	0.22

The strong chemisorption of iodide on the metal surface is responsible for the synergistic effect of iodide ions, in attraction with the BTTPC cation. The BTPPC cation is then adsorbed by the coulombic attraction at the steel surface, where iodide ions are already adsorbed by chemisorption. Stabilization of the adsorbed iodide ions by means of electrostatic interaction with BTPPC leads to greater surface coverage and thereby, greater inhibition. Iofa [38] has shown that I^- alone polarizes both the anodic and cathodic reactions of iron over a wide potential range. It is apparent then that the effects of I^- are not due to electrostatic effects alone, but some covalent bonding to the metal must be involved. The large size and ease of polarizability of I^- facilitates electron pair bonding.

3.3 Adsorption isotherm

Inhibition of corrosion of mild steel in acidic solutions by inhibitors can be explained on the basis of molecular adsorption. Thus, the application of the adsorption isotherm is very useful to study the mechanism of corrosion inhibition. The value of surface coverage (Θ) is obtained by the equation given below:

$$\Theta = I\%/100 \quad (3)$$

Various isotherms were studied for the adsorption of BTPPC + KI on mild steel. On comparing the R^2 values of various isotherms it can be concluded that the adsorption of BTPPC + 10^{-3}M KI on mild steel in 0.3 M H_3PO_4 media follows the Temkin isotherm (R^2 =0.9076). The equation representing the Temkin isotherm [39,40] is given by,

$$e^{-2a\theta} = K.c \quad (4)$$

Taking log on both sides,

$$\theta = -2.303 (\log c)/2a - 2.303 (\log K)/2a \quad (5)$$

where 'a' is the energetic inhomogeneity factor. In this isotherm θ is plotted against log c. From the intercept [-2.303 (log K) /2a], the value of K is calculated and 'a' is given by the slope [-2.303/2a]. The low value of 'a' signifies a weak dependence of the free energy of adsorption on the surface coverage [41,42].

Figure 4 shows the plot of θ against log c for mild steel in 0.3 M H_3PO_4 in the presence of BTPPC + KI at different temperatures.

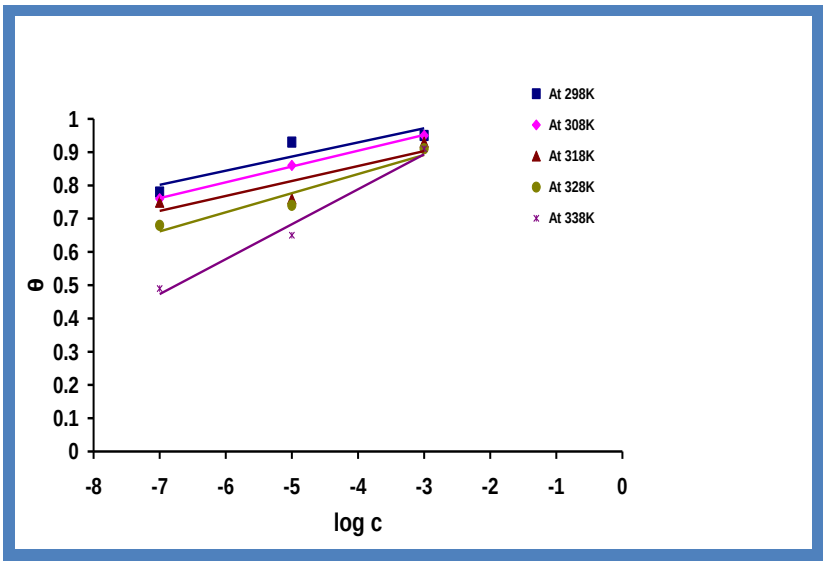

Figure 4. The plot of θ against log c for the Temkin isotherm in the case of BTPPC + KI.

The fraction of surface coverage (θ) shows a linear relationship with log c in Table 6 indicating that adsorption of the compound on the mild steel surface obeys the Temkin's adsorption isotherm [43]. The applicability of the Temkin's adsorption isotherm verifies the assumption of mono-layer adsorption on a uniform, homogeneous metal surface with an interaction in the adsorption layer.

The correlation coefficient is lower than 0.8 at 318 K temperature. This non-uniformity is due to the intrinsic heterogeneity of the surface (edges of crystal growth planes, screw dislocations, kink sites) and to the repulsive forces between adsorbed atoms or molecules.

Table 6. Slope, intercept and correlation coefficient values of the curve between θ versus log c for BTPPC + KI

T / (K)	*Slope*	*Intercept*	R^2
298	0.0425	1.0992	0.8369
308	0.0475	1.0942	0.9991
318	0.0450	1.0383	0.7915
328	0.0575	1.0642	0.9292
338	0.1050	1.2083	0.9815

3.4 Kinetic studies

The effective activation energy is calculated using the following equation given below:

$$\log i_{corr} = B - E_a / 2.303RT \quad (6)$$

Figure 5 shows the graph between log i_{corr} versus 1/T.

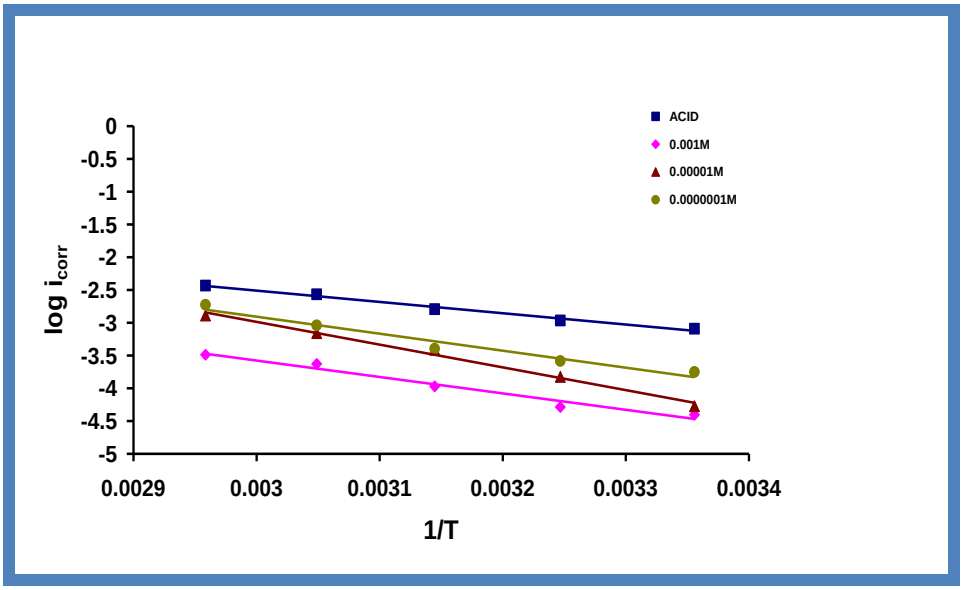

Figure 5. The plot of log i_{corr} against 1/T for mild steel in 0.3 M H_3PO_4 in the presence of BTPPC + KI at different concentrations.

Effective activation energy values are calculated from the slope of these curves and are given in Table 7. The effective activation energy for corrosion of mid steel in 0.3 M H_3PO_4 was found to be 33.07 kJ/mol. In the presence of BTPPC + KI, the average E_a = 54.69 kJ/mol, which is higher compared to pure acid. Hence, BTPPC + KI induces a higher energy barrier and therefore the rate of corrosion decreases.

Table 7. Calculated value of E_a for the corrosion of mild steel in 0.3 M H_3PO_4 in the presence of BTPPC + KI at different concentrations

Conc. / (M)	*Slope*	E_a / (kJ/mol)	R^2
H_3PO_4	-1727.2	33.07	0.9872
10^{-3}	-2502.1	47.91	0.9707
10^{-5}	-3473.4	66.50	0.9907
10^{-7}	-2593.7	49.66	0.9622

The value of E_a lower than 80 kJ/mol indicates physisorption [44]. In the present case E_a in the presence of inhibitor was found to be lower than 80 kJ/mol, therefore the adsorption of BTPPC + KI occurs via physisorption. Since the physical adsorption is proposed, it is expected that there is formation of a protective layer on the surface of mild steel by BTPPC + KI. Table 8 gives various parameters calculated using the Temkin's isotherm.

Table 8. Equilibrium constant and Gibbs free energy values for BTPPC + KI calculated from the Temkin's isotherm

T / (K)	*a*	*K*	$-\Delta G^o_{ads}$ / (kJ/mol)
298	-27.09	7.24×10^{25}	157.50
308	-24.24	1.09×10^{23}	146.15
318	-24.58	1.17×10^{23}	151.08
328	-20.03	3.23×10^{18}	127.19
338	-10.97	3.23×10^{11}	85.77

The value of 'a', the energetic inhomogeneity factor indicates an appreciable dependence of the adsorption enthalpy on the surface coverage θ, for the adsorption of BTPPC + KI on the mild steel. The negative values of ΔG^o_{ads} [45-47] indicate spontaneity of the adsorption process. Gibbs free energy decreases with temperature indicating that the adsorption decreases with a rise in temperature.

3.5 Electrochemical Impedance Spectroscopy (EIS)

The corrosion of mild steel in an acidic solution in the presence of BTPPC + KI was investigated by EIS at 298 K after immersion for 5 h. Double layer capacitance values (C_{dl}) and charge transfer resistance values (R_t) were obtained from impedance measurement. The value of

charge transfer resistance was obtained measuring the diameter of the semicircle and the double layer capacitance was calculated using the following relation:

$$C_{dl} = (2\pi f R_{ct})^{-1} \quad (7)$$

The inhibition efficiency is also calculated using the equation given below:

$$I\% = \left(\frac{R_{ct(i)} - R_{ct(a)}}{R_{ct(i)}} \right) \times 100 \quad (8)$$

where $R_{ct(a)}$ and $R_{ct\ (i)}$ are charge transfer resistance values with and without inhibitor for mild steel in 0.3 M H_3PO_4, respectively, has been determined. It is apparent from Figure 6, as can be seen that the impedance capacitive loop for mild steel in 0.3 M H_3PO_4 solutions changes significantly with increasing inhibitor concentrations. The diameter of the capacitor loop increases tremendously in the presence of inhibitor as compared to that of acid which indicates a high inhibition of corrosion. The largest capacitive loop was obtained for a maximum concentration of inhibitor (10^{-3}M) BTPPC + KI. As the impedance diagrams shown in Figure 6 have an approximately semi-circular [48-50] appearance, it indicates that corrosion of mild steel is mainly controlled by the charge transfer process.

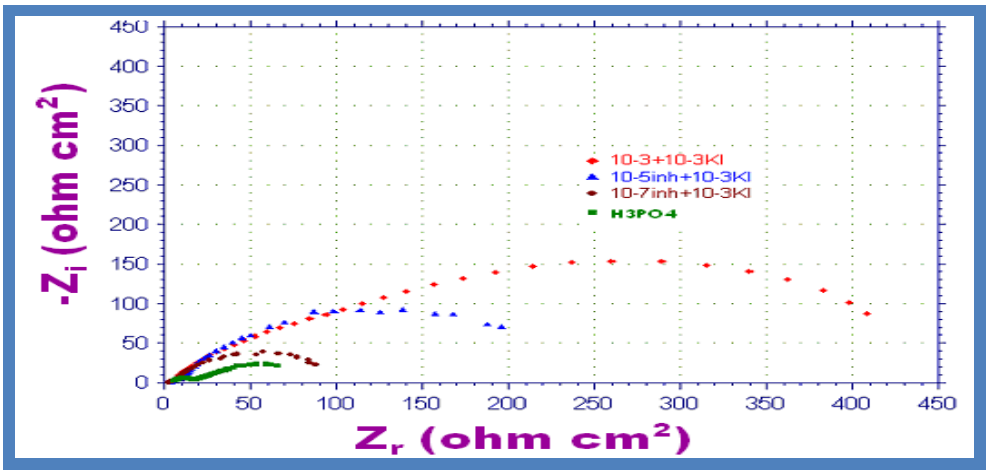

Figure 6. Nyquist plot of mild steel in 0.3 M H_3PO_4 and in the presence of different concentrations of BTPPC + KI at 298 K.

Parameters obtained from EIS and calculated inhibition efficiency (I %) are given in Table 9.

The R_{ct} value was obtained for a maximum concentration of 10^{-3}M BTPPC + KI as 497.8 Ωcm^2. The value of R_{ct} increases in the presence of inhibitor which in turn leads to a decrease in the corrosion current for mild steel in 0.3 M H_3PO_4. Among all the concentrations of BTPPC + KI, 10^{-3} M of BTPPC + KI performs best in 0.3 M H_3PO_4 by enhancing the value of R_{ct} and bringing down the C_{dl} value. Higher values of R_{ct} which arise with higher concentration of BTPPC + KI, is indicative of greater inhibition efficiency.

Table 9. Impedance parameters and inhibition efficiency for the corrosion of mild steel in 0.3 M H_3PO_4 without and with addition of various concentrations of BTPPC + KI at 298 K

Compound	*Conc. /* (M)	R_{ct} / (Ωcm^2)	*f* / (Hz)	C_{dl} / (F/cm^2)	*IE* / (%)
H_3PO_4	0.3	24.449	1.738	$3.75 X10^{-3}$	-
BTPPC + KI	10^{-3}	497.8	3.742	$4.47 X10^{-4}$	95.08
	10^{-5}	257.7	2.105	$8.36 X10^{-4}$	90.51
	10^{-7}	112.2	4.452	$4.48 X10^{-4}$	78.21

The double layer capacitance at the Fe/H_3PO_4 interface decreases with an increase in inhibitor concentration. A decrease in $C_{dl,}$ which can result from a decrease in the local dielectric constant or an increase in the thickness of the electrical double layer, indicates that the inhibitor was adsorbed on the surface at both cathodic and anodic sites. The inhibition efficiencies show an extremely good quantitative correlation.

3.6 Scanning electron microscopy

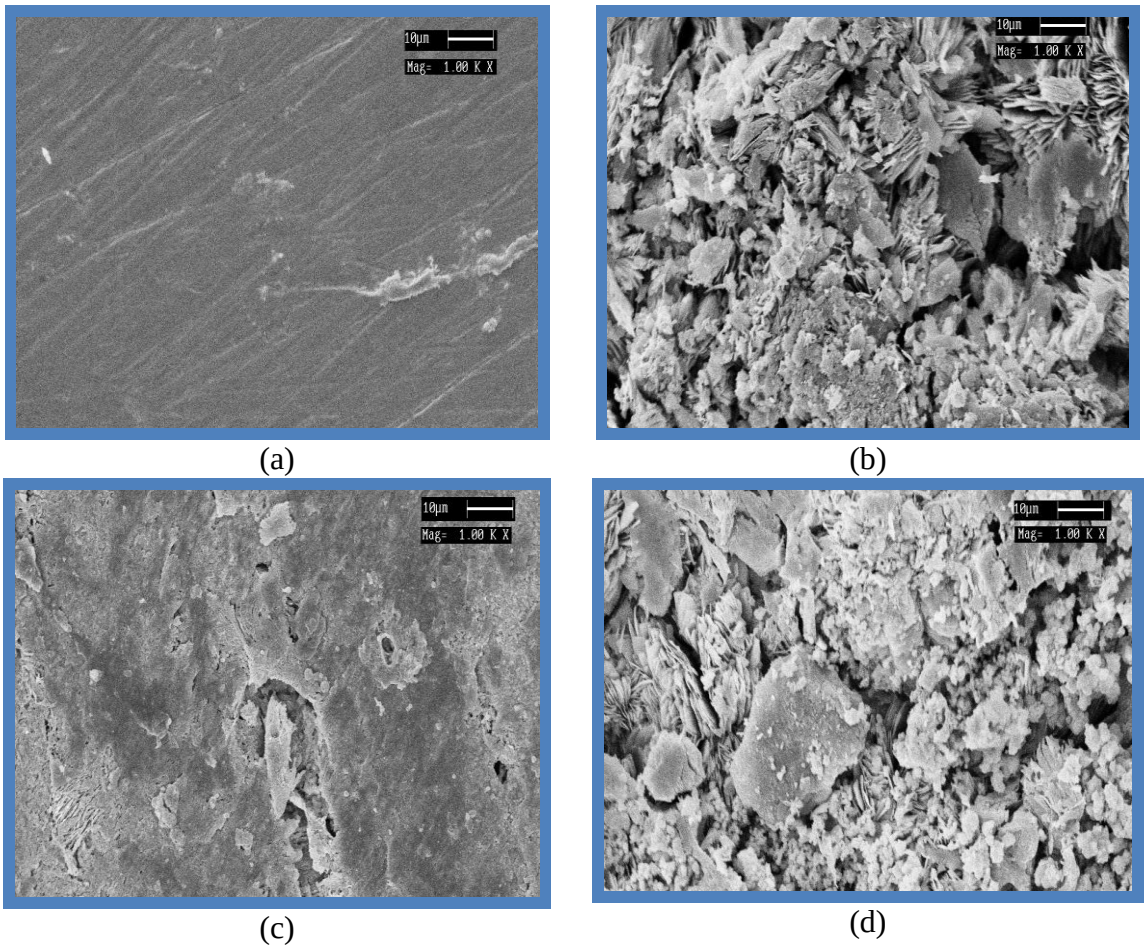

Figure 7. Scanning electron micrograph of (a) plain mild steel surface, (b) Mild steel exposed to 0.3 M H_3PO_4 , (c) mild steel exposed to 0.3 M H_3PO_4 in the presence of 10^{-3} M BTPPC $+10^{-3}$M KI and (d) mild steel exposed to 0.3 M H_3PO_4 in the presence of 10^{-7} M BTPPC + 10^{-3}M KI.

Figures 7 (a) and (b) show the scanning electron micrographs of unexposed specimens of mild steel and mild steel exposed to 0.3 M H_3PO_4. Figures 7 (c) and (d) shows the scanning electron micrographs of mild steel specimens exposed 10^{-3} M BTPPC + KI and 10^{-7} M BTPPC + KI in 0.3 M H_3PO_4.

Figure 7 (a) shows that the surface of the mild steel metal is completely free from any pits and cracks. Polishing scratches are also visible. Flakes can be seen from Figure 7 (b) on the entire mild steel surface when dipped in 0.3 M H_3PO_4 which shows uniform corrosion. From Figure 7 (c) it can be seen that in the presence 10^{-3} M BTPPC + 10^{-3} M KI the metal surface is fully covered with BTPPC + KI and the extent of corrosion in the presence of the highest concentration of inhibitor as visible from micrographs is much less compared to specimens exposed to 0.3 M phosphoric acid. Similar results can be seen from micrographs of the lowest concentration of 10^{-7} M BTPPC + 10^{-3} M KI in Figure 7 (d). Thus these micrographs indicate that BTPPC + KI gives fair amount of protection to mild steel.

3.7 Atomic Force Microscopy

In corrosion inhibition, the inhibitor may form a protective layer on the metal surface. Atomic force microscopy is a method of measuring surface shape and topography on a scale from angstroms to 100 microns. In the present work the average area analysis method is employed to calculate the roughness of the metal surface. In this the entire area of one side of metal surface was considered. After being immersed in 0.3 M H_3PO_4, 10^{-3} M BTPPC + KI and 10^{-7} M BTPPC + KI for 24 hours at room temperature the sample was taken out of the solutions and dried in a desicator for 24 hours. Topographical changes were qualitatively characterized by AFM images. The metal surface could be quantitavely evaluated by measuring the change in the surface roughness and are given in Table 10.

Table 10. Roughness of the Metal surface from atomic force micrographs

Compound	*Conc. /*(M)	*Average Area RMS /* (nm)
H_3PO_4	0.3	65.18
BTPPC + 10^{-3} KI	10^{-3}+ 10^{-3} KI	22.18
	10^{-7}+ 10^{-3} KI	26.50

The RMS value signifies the extent of corrosion i.e. higher the RMS, the more will be the extent of corrosion. Figure 8(a) shows the Atomic Force Micrographs of a plain mild steel specimen whereas Figure 8 (b) shows the Atomic Force Micrographs of a mild steel specimen dipped in 0.3 M H_3PO_4 solution. Figures 8 (c) and 8 (d) show the Atomic Force Micrographs of a mild steel specimen dipped in 10^{-3} M BTPPC + KI and 10^{-7} M BTPPC + KI.

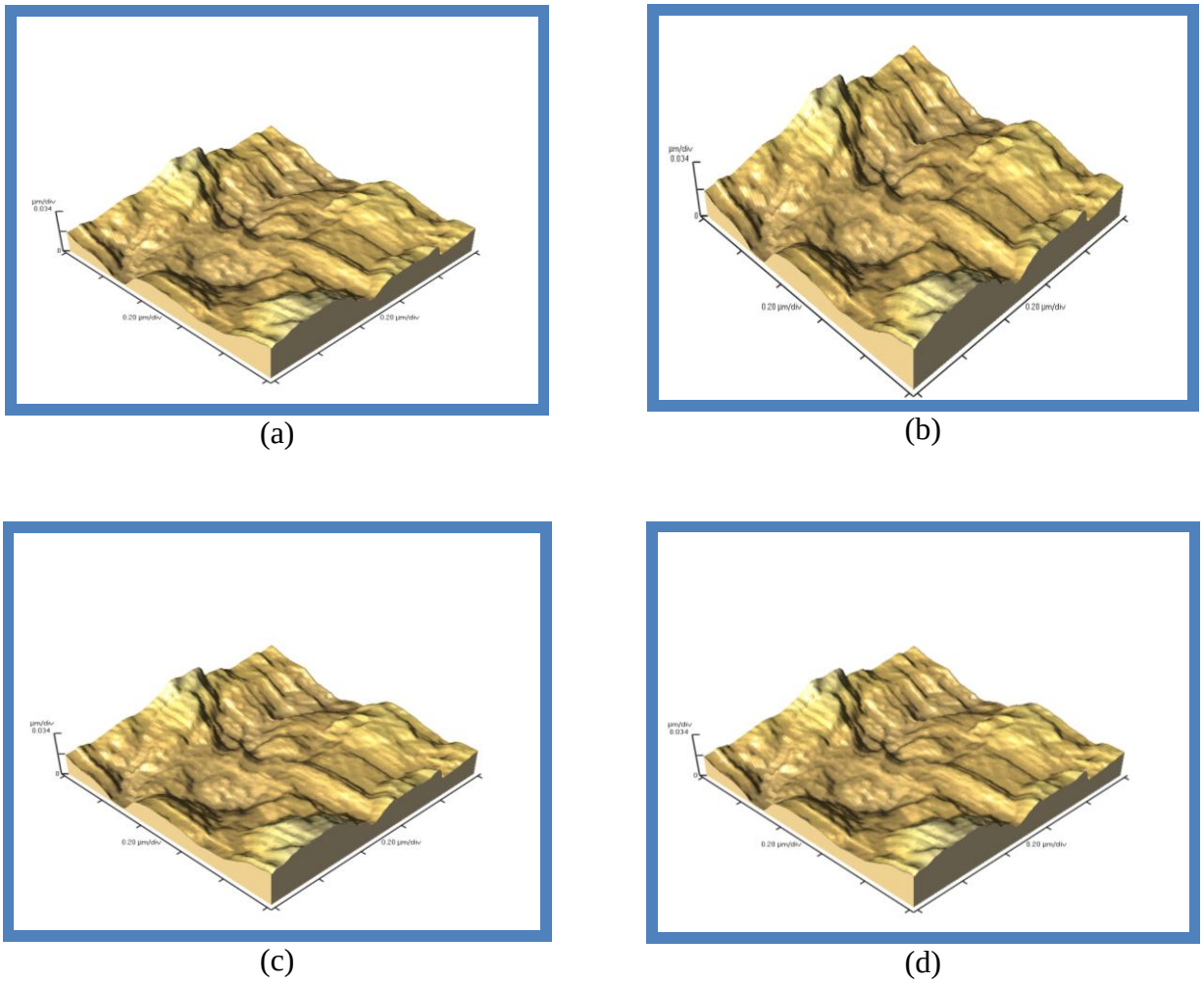

Figure 8. Atomic force microscopy of (a) plain mild steel surface, (b) mild steel specimen in 0.3 M H_3PO_4 , (c) mild steel specimen in 0.3 M H_3PO_4 in the presence of 10^{-3} M BTPPC + 10^{-3}M KI and (d) mild steel specimen in 0.3 M H_3PO_4 in the presence of 10^{-7} M BTPPC + 10^{-3}M KI.

The surface morphology of the plain mild steel indicates there were a few scratches from the mechanical polishing treatment. The mild steel surface was corroded when exposed to H_3PO_4. This can be qualitatively seen from AFM micrographs as there is formation of deep holes and pits. This can be analyzed quantitavely by the RMS value of metal in phosphoric acid as 65.18 nm. The RMS value signifies the extent of corrosion i.e. higher the RMS value the greater will be the extent of corrosion.

4. CONCLUSIONS

The synergistic inhibition between benzyl triphenyl phosphonium chloride and halide ions were investigated. The following conclusions were drawn:

- BTPPC + KI is found to be an excellent inhibitor for mild steel in H_3PO_4.
- The inhibition efficiencies increase with an increase in concentration, but decrease with an increase in temperature for BTPPC + KI.
- E_{corr} remains constant indicating that BTPPC + KI is a mixed type of inhibitor in 0.3 M H_3PO_4 i.e., blocking both cathodic and anodic reactions to an equal extent.
- Adsorption is the only mechanism operative in the case of BTPPC + KI as indicated by b_c and b_a values.
- The adsorption of BTPPC + KI on mild steel is according to the Temkin isotherm in 0.3 M H_3PO_4 media.
- The negative values of ΔG^o_{ads} indicate spontaneity of the adsorption process. ΔG^o_{ads} decreases with temperature in the presence of BTPPC + KI.
- E_a in the presence of BTPPC + KI is higher than compared to pure acid.
- Addition of KI to BTPPC shows a synergistic effect because inhibition efficiencies increase.
- The synergism parameter values (Sθ) show that the corrosion inhibition produced by BTPPC and iodide combination is synergistic in nature.
- The diameter of the capacitor loop increases tremendously in the presence of BTPPC + KI as compared to that of acid which indicates a high inhibition of corrosion.
- The value of R_{ct} (charge transfer resistance) increases in the presence of inhibitor which in turn leads to a decrease in the corrosion current for mild steel in 0.3 M H_3PO_4.
- The C_{dl} double layer capacitance value shows a decrease on the addition of inhibitor as compared to that of acid, indicating a complete film formation on the metal surface in the presence of the inhibitor.
- Surface morphology study (SEM) reveals that the extent of corrosion inhibition is greater at higher concentration as compared to lower concentration.
- AFM micrographs show that the extent of corrosion is highest in 0.3 M H_3PO_4.
- A decrease in the RMS value in the presence of inhibitor shows that BTPPC + KI is a good corrosion inhibitor.

ACKNOWLEDGEMENTS

The authors acknowledge University of KwaZulu-Natal for a postdoctoral scholarship for Dr I. Bahadur.

References

1. L.B. Tang, G.N. Mu, G.H. Liu, *Corros. Sci*., 45 (2003) 2251–2262.
2. P. Manjula, S. Manonmani, P. Jayaram, S. Rajendran, *Anti-Corros. Methods Mater*, 48 (2001) 319–323.
3. F. Bentiss, M. Traisnel, M. Lagrenee, *Br. Corros. J*., 35 (2000) 315–320.
4. B. Mernari, H. El Attari, M. Trainsnel, F. Bentiss, M. Lagrenee, *Corros. Sci*., 40 (1998) 391–399.
5. P. Li, T.C. Tan, J.Y. Lee, *Corrosion*, 53 (1997) 186–194.

6. G. Moretti, G. Quartarone, A. Tassan, A. Zingales, *Electrochim. Acta*, 41 (1996) 1971–1980.
7. S.N. Banerjee, S. Misra, *Corrosion*, 45 (1989) 780–783.
8. F. Bentiss, M. Traisnel, L. Gengembre, M. Lagrenee, *Appl. Surf. Sci*., 61 (2000) 194–202.
9. M.M. Osman, S.S. Abad EL Rehim, *Mater. Chem. Phys*., 53 (1998) 34–40.
10. S. Martinez, I. Stern, *J. Appl. Electrochem*., 31 (2001) 973–978.
11. S.T. Arab, E. A. Noor, *Corrosion*, 49 (1993) 122–129.
12. M.A. Ameer, E. Khamis, G. Al-Senani, *J. Appl. Electrochem*., 32 (2002)149–156.
13. M. El Azhar, B. Mernari, M. Traisnel, F. Bentiss, M. Lagrenee, *Corros. Sci*., 43 (2001) 2229–2238.
14. M.A. Quraishi, D. Jamal, *Corrosion*, 56 (2000) 983–985.
15. B.A. Abd-El-Nabey, E. Khamis, M. Sh. Ramadan, A. El-Gindy, *Corrosion*, 52 (1996) 671–679.
16. F. Bentiss, M. Bouanis, B. Mernari, M. Traisnel, M. Lagrenee, *J. Appl. Electrochem.*, 32 (2002) 671–678.
17. F. Bentiss, M. Traisnel, M. Lagrenee, *Corros. Sci*., 42 (2000) 127–146.
18. S.S. Abd El Rehim, A.M. Magdy Ibrahim, K.F. Khalid, *Mater. Chem. Phys*., 70 (2001) 268–273.
19. M. Lagrenee, B. Mernari, N. Chaibi, M. Traisnel, H. Vezin, F. Bentiss, *Corros. Sci*., 43 (2001) 951–962.
20. E.E. Ebenso. *Mater. Chem. Phys.*, 79 (2003) 58–70.
21. X.H. To, N. Pebere, N. Pelapart, B. Boutevin, Y. Hervaud, *Corros. J*., 35 (2000) 150–154.
22. I. Sekine, Y. Hirakawa, *Corrosion*, 42 (1986) 272–277.
23. E. Khamis, E.S.H. El-Ashry, A.K. Ibrahim, *Br. Corros. J*., 35 (2000) 150–154.
24. Y. Jianguo, W. Lin, V. Otieno-Alego, D.P. Schurinsberg, *Corros, Sci*., 37 (1995) 975–985.
25. E.E. Oguzie, Y. Li, F.H. Wang, *J. Colloid and Interface Sci*., 310 (2007) 90–98.
26. L. Tang, X. Li, G. Mu, L. Li, G. Liu, *Appl. Surf. Sci*., 253 (2006) 2367–2372.
27. M. Bouklah, B. Hammouti, A. Aouniti, M. Benkaddour, A. Bouyanzer, *Appl. Surf. Sci*., 252 (2006) 6236–6242.
28. J.Z. Al, X.P. Guo, J.E. Qu. Z.Y. Chen, J.S. Zhen, *Colloids and Surfaces, A Physicochemical and Engineering Aspects*, 281 (2006) 147–155.
29. C. Jeyaprabha, S. Sattiyanarayanan, G. Venkatachari, *Electrochem. Acta*, 51 (2006) 4080–4088.
30. X. Li, L. Tang, L. Li, G. Mi, G. Liu, *Corros. Sci*., 48 (2006) 308–321.
31. C. Jeyaprabha, S. Sathiyanarayanan, G. Venkatachari, *J. Electroanal. Chem*., 583 (2005) 232–240.
32. A.S. Fouda, H.A. Mastafa, F.K. Taib, G.Y. Elewady, *Corros. Sci*., 47 (2005) 1988–2004.
33. G.N. Mu, X. Li, F. Li, *Mater. Chem. Phys*., 86 (2004) 59–68.
34. E.E. Oguzie, C. Unaegbu, C.N. Ogukwe, B.N. Okolue, *Mater. Chem. Phys.*, 2 (2004) 363–368.
35. H. Vashisht, S. Kumar, I. Bahadur, G. Singh, *Int. J. Electrchem. Sci.*, 9 (2014) 684-699.
36. K. Aramaki, M. Hackerman, *J. Electrochem. Soc*., 116 (1969) 568–574.
37. H. Vashisht, I. Bahadur, S. Kumar, K. Bhrara, D. Ramjugernath', G. Singh, *Int. J. Electrchem. Sci.*, 9 (2014) 2896-2911.
38. Z.A. Iofa, V.V. Batrakov, C.-N.-B. Ba, *Electrochim. Acta*, 9 (1964) 1645–1653.
39. B.R. Babu, R. Holze, *Br. Corros. J*., 35 (2000) 204–209.
40. S. Martinez, I. Stern, *Appl. Surf. Sci*., 199 (2002) 83–89.
41. M.A. Quarishi, D. Jamal, *Corrosion*, 56 (2000) 156–160.
42. M. Sahin, S. Bilgic, *Appl. Surf. Sci*., 147 (1999) 27–32.
43. M.A. Quraishi, D. Jamal, *Corrosion*, 56 (2000) 983–985.
44. S.T. Arab, E.A. Noor, *Corrosion*, 49 (1993) 122–129.
45. A. Popova, E. Sokolova, S. Raicheya, M. Christov, *Corros. Sci*., 45 (2003) 33–58.
46. M. Elachouri, M.S. Hajji, M. Salem, S. Kertit, J. Aride, R. Coudert, E. Essassi, *Corrosion*, 52 (1996) 103–108.
47. E. Khamis, *Corrosion*, 46 (1990) 476–484.
48. S. Martinez, M. Metikos-Hukovic, *J. Appl. Electrochem*., 33 (2003) 1137–1142.

49. H. Ma, X. Cheng, G. Li, S. Chen, Z. Quan, S. Zhao, L. Niu, *Corros. Sci*., 42 (2000) 1669–1683.
50. F. Bentiss, F. Gassama, D. Barbry, L. Gengembre, H. Vezin, M. Lagrenée, M. Traisnel, *Appl. Surf. Sci*., 252 (2006) 2684–2691.